JOURNAL OF CATALYSIS 156, 298–300 (1995)

# NOTE

# New Layered Vandyl(IV) Phosphite as a Precursor to Vanadyl Pyrophosphate Catalysts for Partial Oxidation of *n*-Butane to Maleic Anhydride

The discovery of the vanadium–phosphorus–oxide system as a catalyst for selective oxidation of *n*-butane to maleic anhydride has prompted research into the synthesis of new vanadium phosphate phases. The most selective partial oxidation catalysts have been associated with vanadyl(IV) pyrophosphate, $(VO)_2P_2O_7$, formed by the dehydration of vanadyl(IV) hydrogen phosphate hemihydrate, $VOHPO_4 \cdot 0.5H_2O$. The structural similarity between vanadyl pyrophosphate and its pyrolitic precursor is manifested in the presence of vanadyl dimers in both structures connected through corners by $P_2O_7$ or $HPO_4$ groups, respectively. The catalytic properties of vanadyl pyrophosphate have been associated with the $V_2O_8$ dimers on its basal plane (the (200) plane) exposed to the gas phase reactants (1).

The synthesis and characterization of layered vanadyl(IV) phosphonates, $VOC_nH_{2n+1}PO_3 \cdot xH_2O$, containing the $V_2O_8$ dimers have been recently reported (2–4). We present here the results of partial oxidation of *n*-butane on VPO catalysts derived from the simplest of these phosphonates, vanadyl phosphite. The results indicate that vanadyl(IV) phosphite is the precursor to vanadyl pyrophosphate catalysts with high surface area (ca. 45 $m^2/g$) and selectivity to maleic anhydride in *n*-butane partial oxidation comparable to the conventional unpromoted catalyst.

The synthesis and characterization of vanadyl(IV) phosphite have been described in detail elsewhere (2–4). Typically, vanadium pentoxide (Aldrich) was refluxed in adhydrous ethanol (Aldrich) for 16 h to reduce the vanadium. Phosphorous acid (Aldrich) dissolved in anhydrous ethanol was added to give a P/V ratio of 1.0–1.3, and the reaction mixture was refluxed for another 20 h. A light blue solid was separated by filtration, washed with ethanol and acetone, and dried in air.

Vanadyl(IV) phosphite was also synthesized using a V(IV) source, such as vanadyl(IV) acetylacetonate. $VO(acac)_2$ (Aldrich) was added to phosphorous acid (P/V = 1.2) dissolved in anhydrous ethanol and refluxed for 2 days. The light blue solid was separated by filtration, washed with ethanol and acetone, and dried in air.

Powder X-ray diffraction patterns of both the vanadyl phosphite and the activated catalysts were recorded with a Scintag/USA DMS 2000 diffractometer using Cu$K\alpha$ radiation. The XRD pattern of vanadyl phosphite is shown in Fig. 1a This low crystalline pattern most likely corresponds to either an orthorhombic or a monoclinic unit cell (3). Unfortunately, we have not been able to obtain vanadyl phosphite crystals of sufficient quality for single crystal structural analysis.

The results of the elemental analysis showed that the bulk P/V ratios in vanadyl phosphite depended on the P/V ratio during the synthesis (Table 1). At the same time, the surface P/V ratio was independent of synthesis P/V ratios, which is opposite to the case of the $VOVHPO_4 \cdot 0.5H_2O$ precursor (1). The elemental analysis was consistent with a formula of vanadyl phosphite, $VOHPO_3 \cdot 1.5H_2O$. The formula agreement is not exact. The material as synthesized was a powder with surface areas of 13–20 $m^2/g$, which could adsorb up to 10 mol% water. Differences in termination of the surface with phosphite or vanadyl groups may also contribute a variation to the P/V ratio. X-ray photoelectron spectroscopy (XPS) of the sample showed a P(2*p*) binding energy of 133.4 eV, consistent with a $P^{III}$ species (6a). This P(2*p*) binding energy is 0.6–0.7 eV lower than observed for $P^V$ species, e.g., in $VOHPO_4 \cdot 0.5H_2O$ (6b). The XPS data also indicated surface enrichment of phosphorus, which is common to most vanadium phosphate catalysts (6b).

Vanadyl(IV) phosphite samples derived from both the V(V) and V(IV) sources displayed the same XRD pattern, Ramen, and IR spectra. Although some oxidation of the $P^{III}$ to $P^V$ by $V^V$ during the synthesis cannot be ruled out completely, the elemental analysis, XPS, XRD, Raman, and IR data strongly support the formation of phosphite (3). Apparently, the rate of $V^V$ reduction by alcohol molecules in anhydrous alcohol is considerably higher than the rate of $V^V$ reduction by the phosphite at low acidity (7), which may explain why $P^{III}$ is not oxidized.

Low temperature magnetic susceptibility behavior of vanadyl(IV) phosphite indicated the antiferromagnetically exchange-coupled vanadyl dimers (3) associated with the presence of $V_2O_8(H_2O)$ dimers in the solid state structure (8). Vanadyl(IV) phosphite is converted to vanadyl pyrophosphate when heated in an oxygen-containing atmo-



0021-9517/95 $12.00

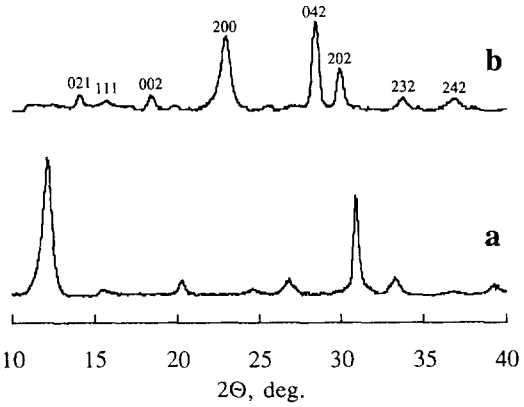


FIG. 1. X-ray diffraction patterns of (a) vanadyl(IV) phosphite (P/V = 0.93) and (b) the corresponding catalyst, with peaks indexed to $(VO)_2P_2O_7$.

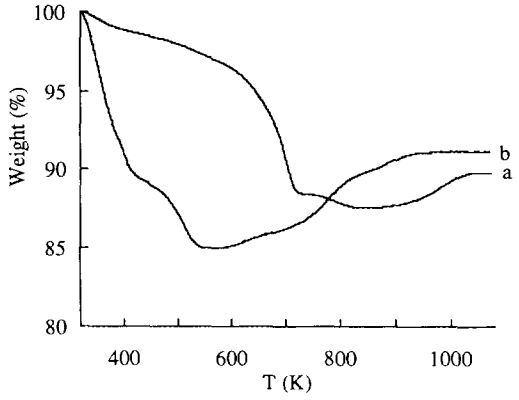


FIG. 2. TGA curves of (a) $VOHPO_4 \cdot 0.5H_2O$ and (b) $VOHPO_3 \cdot 1.5H_2O$ (P/V = 0.93) in air. Heating rate: 10 K/min.

sphere, offering further support that the presence of the vanadyl dimers is the key to creating the structure of vanadyl pyrophosphate.

The TGA curve of vanadyl phosphite (10 K/min in air) shows a multistep weight loss in the 320–570 K range and weight gain in the 570–970 K range (Fig. 2b). The overall weight loss in the 320–570 K range corresponds to the loss of intercalated and structural water, oxidation of P—H into P—OH, and formation of the pyrophosphate groups accompanied by evolution of water. Transformation to vanadyl pyrophosphate is complete by 520 K (Fig. 2b), while temperatures of at least 150 K higher are generally needed to transform $VOHPO_4 \cdot 0.5H_2O$ precursors (Fig. 2a).

The structural and intercalated water in the phosphite is involved in a weak interlayer bonding interaction with vanadyl groups. In contrast, the structural water in $VOHPO_4 \cdot 0.5H_2O$ forms strong hydrogen bonds with the P-OH groups in adjacent layers. These weak interlayer interactions are key to the facile removal the water. The weight loss in the 300–520 K range corresponds to the combined processes of dehydration and partial oxidation:

$$2VOHPO_3 \cdot 1.5H_2O + O_2 = (VO)_2P_2O_7 + 4H_2O.$$

TABLE 1

**Bulk P/V Ratios in Vanadyl Phosphite ($VOHPO_3 \cdot 1.5H_2O$) with Different Synthesis P/V Ratios**

| | $(P/V)_{init}$ = 1.00 | $(P/V)_{init}$ = 1.17 | $(P/V)_{init}$ = 1.30 |
|---|---|---|---|
| $(P/V)_{bulk}$ | 0.85 | 0.93 | 1.15 |
| O/P (XPS) | 4.3 | 4.3 | 4.2 |
| P/V (XPS) | 1.54 | 1.57 | 1.59 |
| P(2*p*), eV | 133.6 | 133.4 | 133.4 |

The weight gain in the 570–970 K range corresponds to the process of further oxidation of vanadyl pyrophosphate into vanadyl(V) orthophosphate, $\alpha_1$-$VOPO_4$, which takes place at higher temperatures.

Oxidation of *n*-butane was carried out using ca. 1 g of vanadyl(IV) phosphite sieved to 35–65 mesh. The phosphite was placed into a U-tube Pyrex glass reactor inside an aluminum split block and activated in 1.2% *n*-butane in dry air at space velocity of 400 $h^{-1}$ in two steps: first at 593 K for 1 day, and then at 708 K for 6 days. Similar activation produced the most selective catalysts from $VOHPO_4 \cdot 0.5H_2O$ precursors (5). Kinetic data were collected at 654 K in 1.2% *n*-butane in air. All experiments were carried out in once-through integral mode. CP grade *n*-butane from Matheson and dry air were metered separately using Brooks Model 52-36A1V Series mass flow controllers with Model 5876 two-channel power supply box and mixed in desired proportions. Only a small fraction of the total flow was metered to the reactor; the rest was vented.

The effluent stream was analyzed by on-line gas chromatography. The lines from the reactor to gas chromatographs were kept at 420 K to prevent condensation of maleic anhydride. A side stream ran from the heated effluent line to a HP 5790A Series gas chromatograph where partial oxidation products (mainly MA and traces of acetic and acrylic acids) were separated on a 2 m long Porapak QS column. The bulk of the reactor effluent was directed through a water bubbler that stripped the partial oxidation products. The effluent samples from a sample loop were then injected into two GC columns in series: a 5 m long 30% bis-2-ethoxyethyl sebacate column to separate $CO_2$ and butane, and a 4 m long molecular sieve 13X column to separate $O_2$, $N_2$, and CO.

Three samples of vanadyl phosphite with different P/V ratios activated in the flow reactor produced dependence

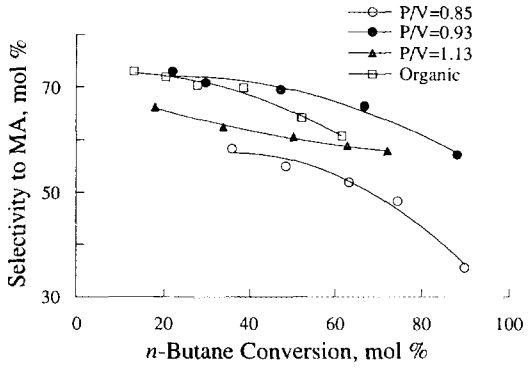


FIG. 3. Selectivity to maleic anhydride vs *n*-butane conversion of 654 K in 1.2% *n*-butane–air for VPO catalysts produced from vanadyl(IV) phosphite samples with the bulk P/V ratios of 0.85, 0.93, and 1.13 and the organic $VOHPO_4 \cdot 0.5H_2O$ precursor possessing synthesis P/V of 1.18 (9).

of selectivity to maleic anhydride on *n*-butane conversion, shown in Fig. 3. For comparison, the selectivity–conversion relationship for a sample of conventional organic (unpromoted) catalyst (9), displaying the best selectivity which was prepared and tested in our laboratory, is also shown. The P/V = 0.93 vanadyl phosphite sample exhibited considerably higher selectivities than the organic catalyst at *n*-butane conversions above 40% (Fig. 3). After the kinetic runs the BET surface area of the P/V = 0.85 and 1.13 vanadyl phosphite samples were 40.9 and 43.4 $m^2/g$, while the most selective P/V = 0.93 sample had a surface area of 37.7 $m^2/g$. These values are high for the VPO system where surface areas are generally less than 20 $m^2/g$. The BET surface areas of the unpromoted organic catalyst employed were found to be 11.3 $m^2/g$. The XRD pattern of the P/V = 0.93 vanadyl phosphite catalyst (Fig. 1b) shows the presence of only crystalline vanadyl(IV) pyrophoshate.

The use of vanadyl(IV) phosphite was motivated by the similarity in structure with the conventional $VOHPO_4 \cdot 0.5H_2O$ (hemihydrate) precursor. The transformation of $VOHPO_4 \cdot 0.5H_2O$ into a selective vanadyl pyrophosphate catalyst relies on the existence of vanadyl dimers in both structure (1). Our previous work based on XRD, elemental analysis, vibrational spectroscopy, magnetic susceptibility, and intercalation of *n*-alkylamines suggests that $VOHPO_3 \cdot 1.5H_2O$ also contains vanadyl dimers and is structurally similar to $VOHPO_4 \cdot 0.5H_2O$ (4, 10).

Vanadyl pyrophosphate catalysts prepared from vanadyl(IV) phosphite precursors manifest better selectivity toward maleic anhydride during the partial oxidation of *n*-butane. Activation of vanadyl phosphite can be carried out at lower temperatures, which can reduce the possibility of overoxidation to vanadium orthophosphate, which is detrimental to VPO catalyst performance. Another advantage of the vanadyl phosphite precursor to vanadyl pyrophosphate is that it yields catalysts possessing greater surface area than the conventional unpromoted VPO catalysts.

## ACKNOWLEDGMENTS

This work was supported by the AMOCO Chemical Corporation and National Science Foundation Grant CTS-9100130. The authors thank Drs. John M. Forgac, Muin S. Haddad, and Hassan Teheri of AMOCO Chemical Corporation for the XPS data and many helpful discussions.

## REFERENCES

1. Cavani, F., and Trifirò, F. *Catalysis* **11,** 246, (1994); and refs. therein.
2. Guliants, V. V., Benziger, J. B., and Sundaresan, S., "*Vanadyl Pyrophosphate Precursors.*" U.S. Patent application 08/338,237, filed November 14, 1994.
3. Guliants, V. V., Benziger, J. B., and Sundaresan, S., *Chem. Mater.* **7,** 1485 (1995).
4. Guliants, V. V., Benziger, J. B., Sundaresan, S., and Wachs, I. E., *Chem. Mater.* **7,** 1493 (1995).
5. Buchanan, J. S., and Sundaresan, S., *Appl. Catal.* **26,** 211 (1986).
6. (a) Moulder, J. F., Stickle, W. F., Sobol, P. E., and Bomben, K. D., *in* "Handbook of X-ray Photoelectron Spectroscopy" (J. Chastain, Ed.). Perkin–Elmer Corporation, Eden Prairie, MN, 1992; (b) Zazhigalov, V. A., Haber, J., Stoch, J., Pyatnitskaya, A. I., Komashko, G. A., and Belousov, V. M., *Appl. Catal. A* **96,** 135 (1993).
7. (a) Waters, W. A., and Littler, J. S., *in* "Oxidation in Organic Chemistry" (K. B. Wilberg, Ed.), Part A, p. 185. Academic Press, New York, 1965; (b) Rocek, J., and Aylward, D. E., *J. Am. Chem. Soc.* **97,** 5452 (1975); (c) Horowitz, H. S., Blackstone, C. M., Sleight, A. W., and Teufer, G., *Appl. Catal.* **38,** 193 (1988).
8. Huan, G., Johnson, J. W., Brody, J. F., and Goshorn, D. P., *Mater. Chem. Phys.* **35,** 199 (1993).
9. Milberger, E. C., Bremer, N. J., and Dria, D. E., U.S. Patent 4,333,853 (1982).
10. Guliants, V. V., Benziger, J. B., and Sundaresan, S., *Chem. Mater.* **6,** 353 (1994).

V. V. Guliants*
J. B. Benziger†,[1]
S. Sundaresan†

*Departments of *Chemistry and †Chemical Engineering*
*Princeton University*
*Princeton, New Jersey 08544*

Received February 7, 1995; revised May 25, 1995; accepted July 20, 1995

[1] To whom correspondence should be addressed. E-mail: benziger@princeton.edu.